



Measurements of Gamma-Ray Emission Cross Sections and Angular Distributions from $(n, X\gamma)$ Reactions of 14.1 MeV Neutrons with O, Cl, K, Ca, Ti, Cr, Fe, and Ni nuclei

D.N. Grozdanov for TANGRA collaboration



The work was carried out with the financial support of the RSCF (grant No. 23-12-00239).

Elements	Importance for Neutron-Nuclear Physics and Nucleosynthesis	Importance for Nuclear Reactor Technology
Carbon (C), Oxygen (O), Magnesium (Mg)	<ul style="list-style-type: none"> ● Helps in understanding nuclear forces, interactions, and reaction mechanisms. ● Plays a crucial role in stellar nucleosynthesis, particularly in forming heavier elements through fusion processes. ● Fundamental to the study of quantum mechanics and particle physics, aiding in the understanding of matter and energy interactions. 	<ul style="list-style-type: none"> ● Essential for slowing down fast neutrons, improving reactor efficiency. ● Key for optimizing neutron moderation and reactor design. ● Investigates structural integrity under neutron exposure. ● Important in fusion processes, particularly in plasma containment and stability. ● Used in molten salt reactors for heat transfer and chemical stability.
Chromium (Cr), Iron (Fe), Nickel (Ni)	<ul style="list-style-type: none"> ● Important for investigating neutron interactions, capture processes, and reaction cross-sections involving heavier elements. ● Contributes to nucleosynthesis processes in stars and supernovae, aiding in the formation of heavier elements. ● Essential for understanding the behavior of materials under extreme conditions, linking to fundamental physics principles. 	<ul style="list-style-type: none"> ● Improves safety and performance of materials under neutron bombardment. ● Assesses material longevity and performance under neutron exposure. ● Enhances mechanical properties and corrosion resistance of reactor materials. ● Important for structural components in fusion reactors and molten salt reactors.

Elements	Importance for Neutron-Nuclear Physics and Nucleosynthesis	Importance for Nuclear Reactor Technology
Calcium (Ca), Chlorine (Cl)	<ul style="list-style-type: none"> Contributes to understanding nuclear reactions involving light nuclei and the behavior of halogens in nuclear processes. Plays a role in nucleosynthesis in stars, although not primarily involved in fission or fusion. Important for studying fundamental interactions and decay processes, enhancing knowledge of atomic structure. 	<ul style="list-style-type: none"> Critical for designing effective shielding solutions in nuclear applications. Provides insights into the chemical behavior of chlorine in nuclear contexts, aiding in waste management strategies. Plays a role in the chemistry of molten salt reactors, enhancing safety and efficiency.
Potassium (K)	<ul style="list-style-type: none"> Important for investigating neutron interactions, capture processes, and reaction cross-sections involving heavier elements. Contributes to nucleosynthesis processes in stars and supernovae, aiding in the formation of heavier elements. Essential for understanding the behavior of materials under extreme conditions, linking to fundamental physics principles. 	<ul style="list-style-type: none"> Important for health physics and radiation safety research. Improves analytical methods for trace element detection in various fields. Can be used in molten salt reactors for heat transfer and as a tracer in fusion studies.

Cross-section data sources $^{12}\text{C}(\text{n},\text{n}'\gamma)_{4439\text{keV}}^{12}\text{C}$

4439	$^{12}\text{C}(\text{n},\text{n}')^{12}\text{C}$	$4439(2^+) \rightarrow 0(0^+), \text{p}$
------	--	--

14.2

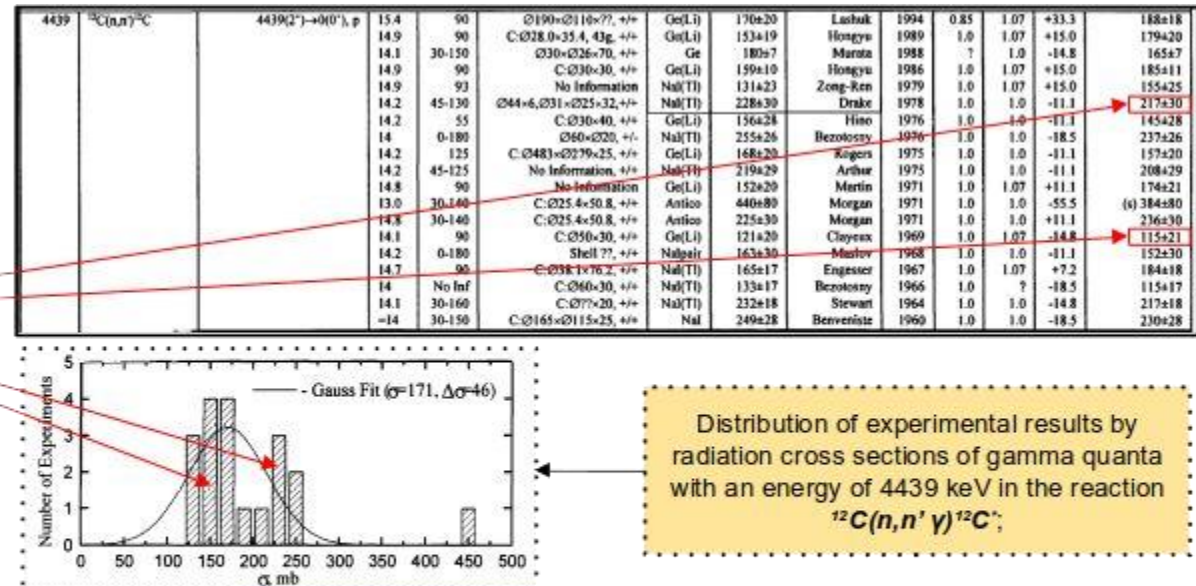
14.1

[MeV]

15.4	188±18
14.9	179±20
14.1	165±7
14.9	185±11
14.9	155±25
14.2	217±30
14.2	145±28
14	237±26
14.2	157±20
14.2	208±29
14.8	174±21
13.0	(s) 384±80
14.8	236±30
14.1	115±21
14.2	152±30
14.7	184±18
14	115±17
14.1	217±18
=14	230±28

217 ± 30

115 ± 21
[mb]



The discrepancy is two times!!!

<https://inis.iaea.org/records/c44gw-yfn27>

Nowadays, the most complete collection of data on reaction cross sections ($n, n' \gamma$) for neutrons with an energy of 14.5 MeV is presented in INDC(CCP)-413 (*Status of experimental and evaluated discrete γ -ray production at $E_n = 14.5$ MeV*) 1998.

Distribution of experimental results by radiation cross sections of gamma quanta with an energy of 4439 keV in the reaction $^{12}\text{C}(n, n' \gamma)^{12}\text{C}$.

Cross-section data sources $^{48}\text{Ti}(\text{n},\text{n}'\gamma_{984\text{keV}})^{48}\text{Ti}$

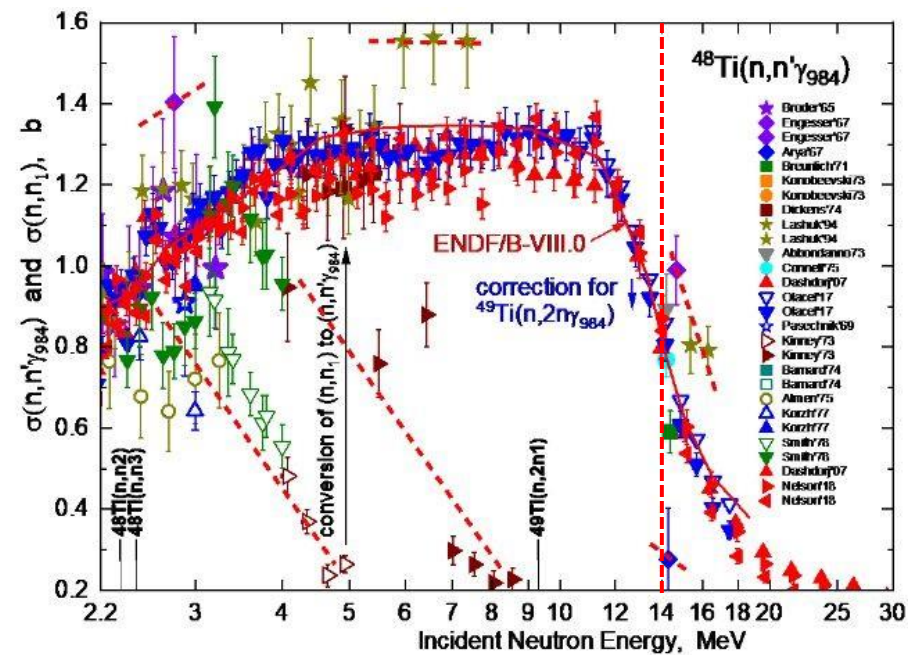


<https://doi.org/10.61092/iaea.y3q8-a4b5>

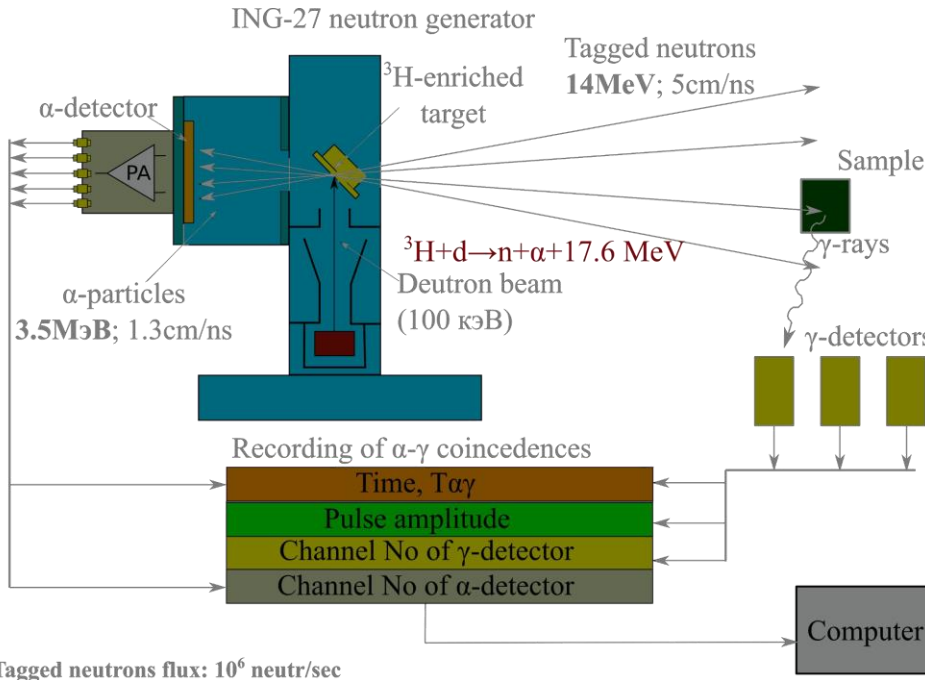
INDC(NDS)-0740
Distr. ST, G

INDC International Nuclear Data Committee

Evaluation of the $^{48}\text{Ti}(\text{n},\text{n}'\gamma_{984\text{keV}})$ γ -ray production cross section for standards

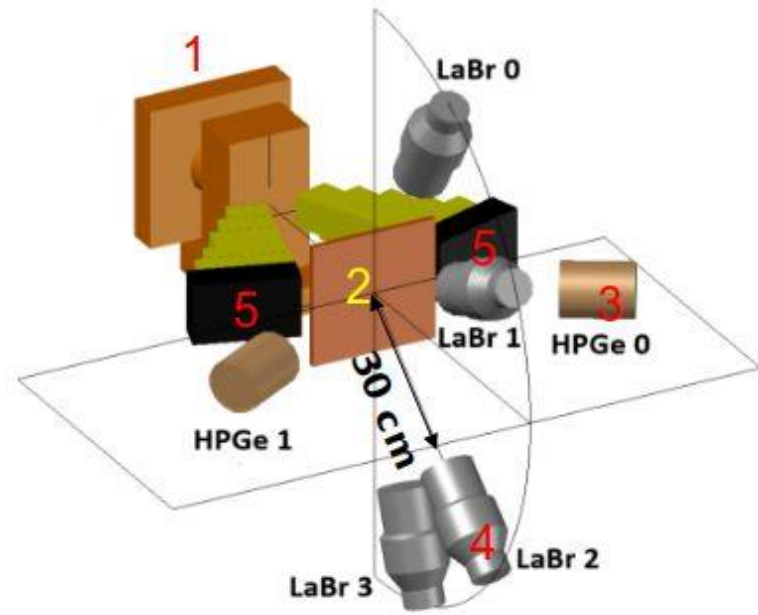


The tagged neutron method (TNM) & TANGRA setup



Interesting for nuclear reactions research:

- Angular distributions of n and γ
- Correlation between n and γ



1. ING-27 neutron generator
2. Sample 20×20×X cm
3. HPGe γ -detector (2 pcs, 60% eff)
4. LaBr₃ detector (4 pcs)
5. Collimator (Fe + Pb)

Sample characteristics

Sample	Density (g/cm ³)	Size (cm ³)	Isotopic composition
CH ₂ Cl ₂	1.294	20 x 20 x 4	¹² C - 98.9%, ³⁵ Cl - 75.8%, ³⁷ Cl - 24.2%
KCl	1.254	20 x 20 x 4	³⁹ K - 93.3%, ⁴¹ K - 6.7%, ³⁵ Cl - 75.8%, ³⁷ Cl - 24.2%
CaO	0.628	20 x 20 x 4	⁴⁰ Ca - 96.9%, ⁴⁴ Ca - 2.1%, ¹⁶ O - 98.7%
TiO ₂	0.878	20 x 20 x 4	⁴⁶ Ti - 8.3%, ⁴⁷ Ti - 7.4%, ⁴⁸ Ti - 73.7%, ⁴⁹ Ti - 5.4%, ⁵⁰ Ti - 5.2%, ¹⁶ O - 98.7%
Cr ₂ O ₃	2.081	20 x 20 x 2	⁵⁰ Cr - 4.3%, ⁵² Cr - 83.8%, ⁵³ Cr - 9.5%, ⁵⁴ Cr - 2.4%, ¹⁶ O - 98.7%
Fe	3.629	20 x 20 x 2	⁵⁴ Fe - 5.8%, ⁵⁶ Cr - 81.8%, ⁵⁷ Fe - 2.1%
Ni ₂ O ₃	2.070	20 x 20 x 2	⁵⁸ Ni - 68.1%, ⁶⁰ Ni - 26.2%, ⁶² Ni - 3.6%, ¹⁶ O - 98.7%

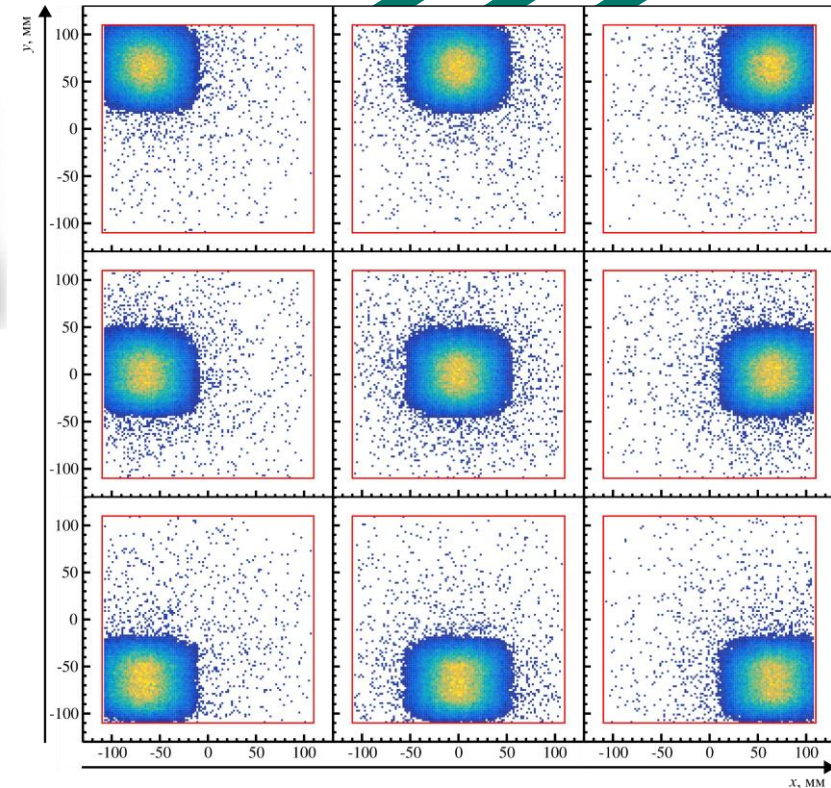
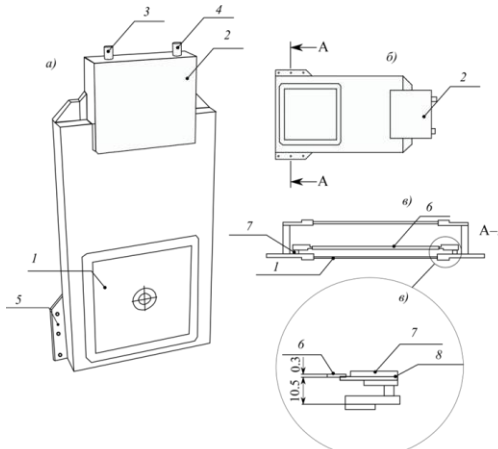
Measurement of “tagged” neutron beam profiles

2D-detector, made of 4 double-sided stripped position-sensitive Si-detectors



Each Si detector consists of 32x32 strips ~ 1.8 mm thick
Size of one detector:
 60×60 mm 2

Total size: 120x120 mm 2 Thickness: 0.3 mm Neutron detection efficiency: $\sim 0.8\%$



Data processing: Time spectra

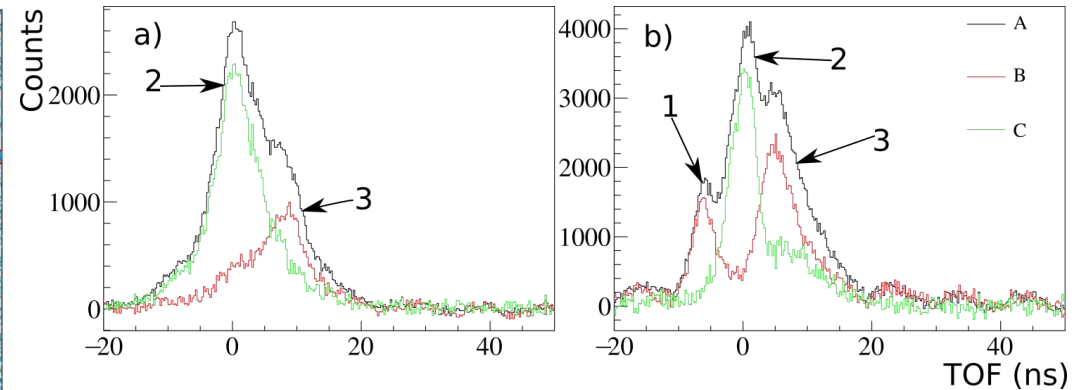
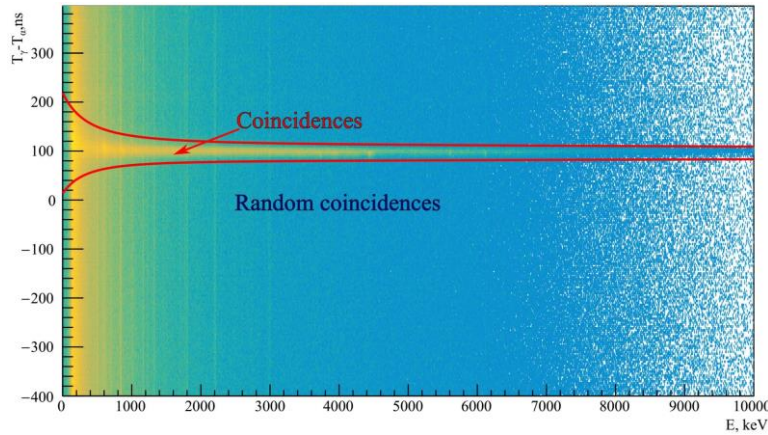
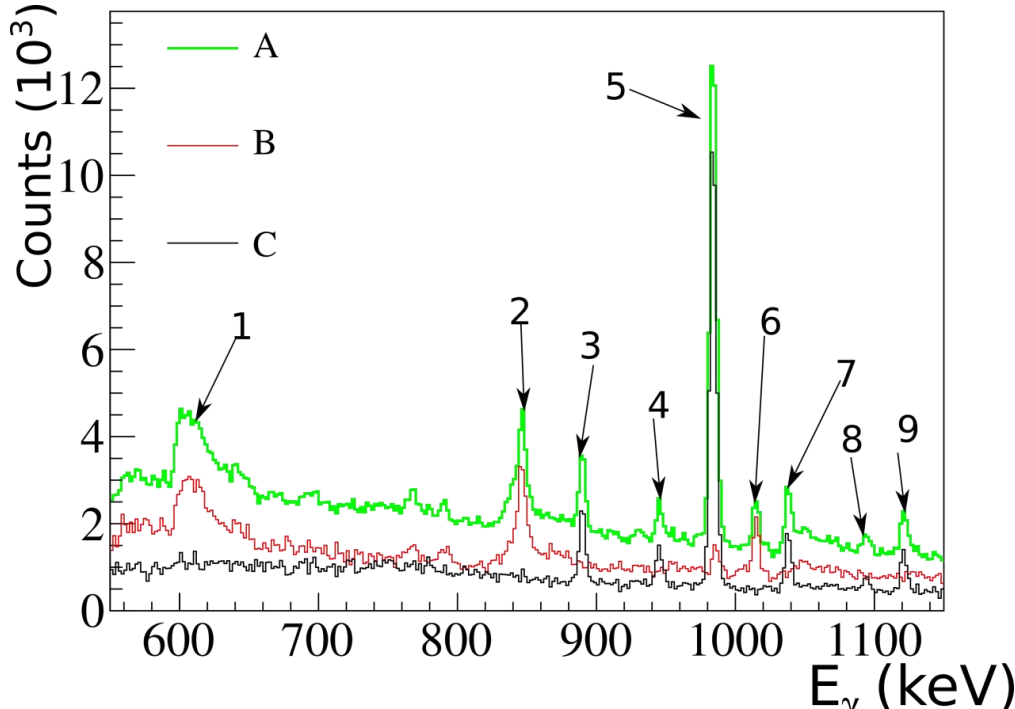


Diagram energy (E_γ) – the time between the registration of a γ -quantum and its corresponding α -particle ($T_\gamma - T_\alpha$) formed as a result of reactions in the sample, with a highlighted coincidence window.

Example of time spectra (in the energy window of about 1 – 2 MeV) for HPGe detector a) and LaBr detector b).

Where: A – With sample, B – Without sample, C – Difference. 1 – is γ -from (Fe – Pb) - Collimator, 2 – γ from sample, 3 – is scattered neutrons

Data processing: Energy spectra



A – with sample, B – without sample,

C – difference (net spectrum).

No	$E\gamma$ (keV)	Reaction
1	600	$^{72}\text{Ge}(\text{n},\text{n}'\gamma)$
2	846	$^{56}\text{Fe}(\text{n},\text{n}'\gamma)$
3	889	$^{46}\text{Ti}(\text{n},\text{n}'\gamma)$
4	944	$^{46}\text{Ti}(\text{n},\text{n}'\gamma)$
5	983	$^{48}\text{Ti}(\text{n},\text{n}'\gamma)$
6	1014	$^{27}\text{Al}(\text{n},\text{n}'\gamma)$
7	1037	$^{48}\text{Ti}(\text{n},\text{n}'\gamma)$
8	1092	$^{47}\text{Ti}(\text{n},\text{n}'\gamma)$
9	1120	$^{46}\text{Ti}(\text{n},\text{n}'\gamma)$

Cross section calculation

$$\frac{d\sigma}{d\Omega}(\theta) = \frac{N_p \cos \xi}{4\pi N_\alpha n_{at} k} 10^{27} \left[\frac{\text{mbarns}}{\text{sr}} \right]$$

Area of γ -peak Incident angle
 Number of tagged neutrons Surface density of atoms in the sample

- The features of the experimental approach include a close geometry and a relatively large sample.
- All corrections change significantly depending on the target thickness.
- We could not consider the various corrections independently.

Total reaction cross section

$$\sigma = 2\pi \int_{-1}^1 \frac{d\sigma}{d\Omega} (\cos\theta) d\cos\theta$$

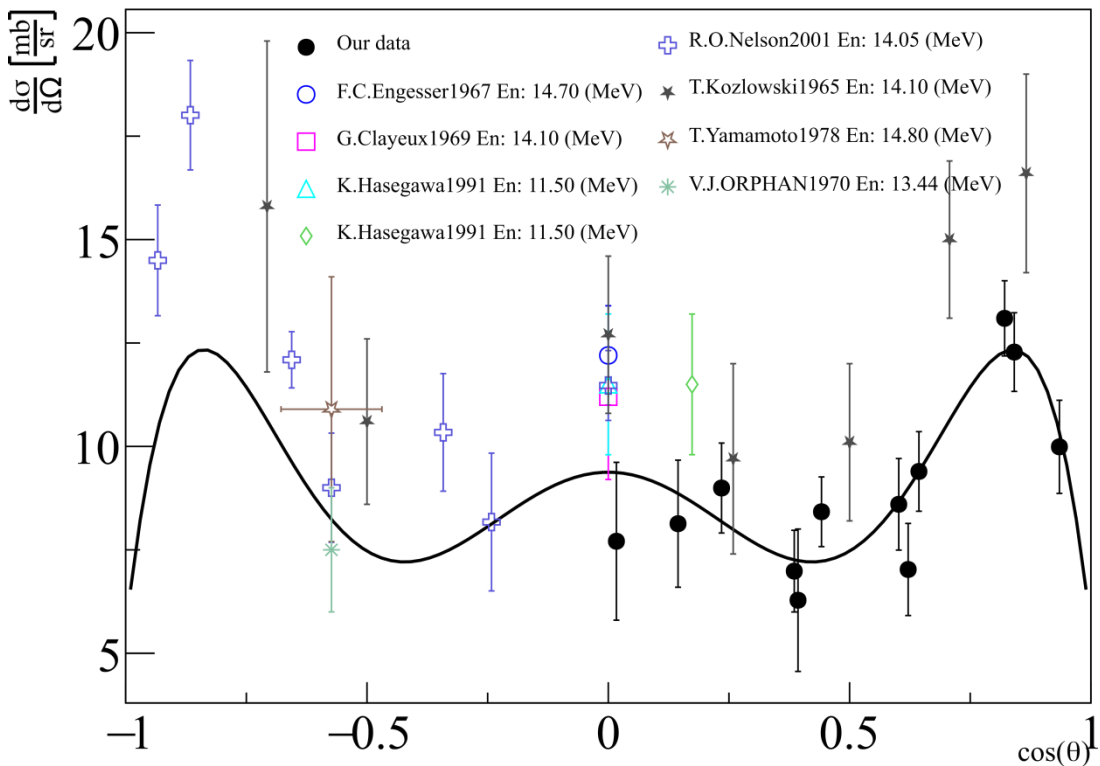
Multiple inelastic scattering Change in incident neutron number
 Sample thickness Attenuation of γ -rays
 The total efficiency

$$k = \int_0^{x_0} \varepsilon(x) k_{ms}(x) k_{satt}(x) k_{iatt}(x) dx$$

Results of cross-section measurements for oxygen

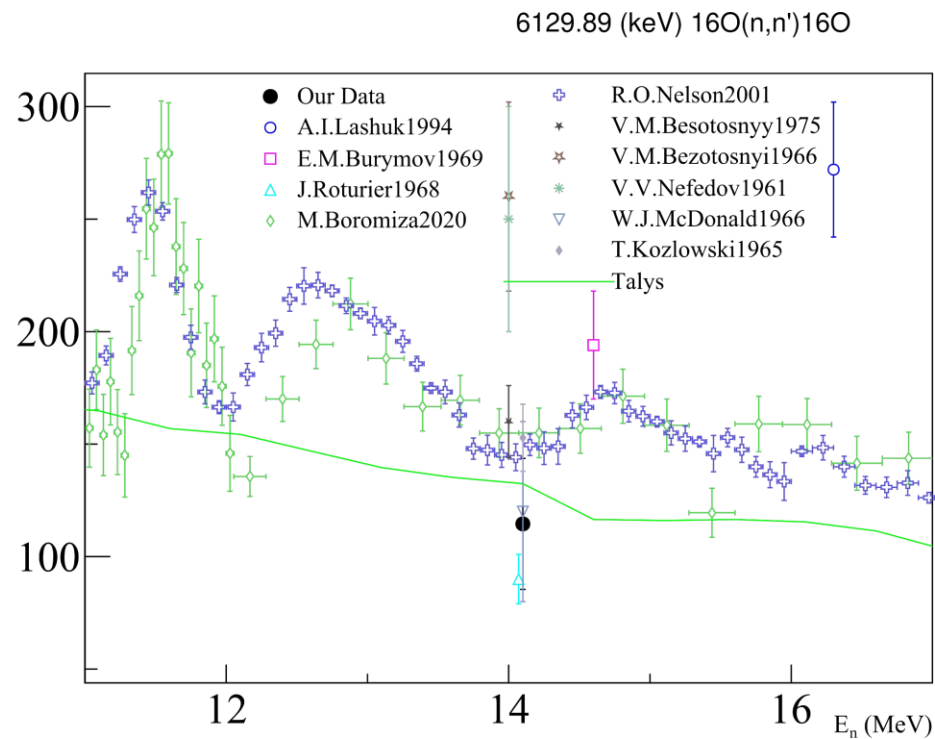
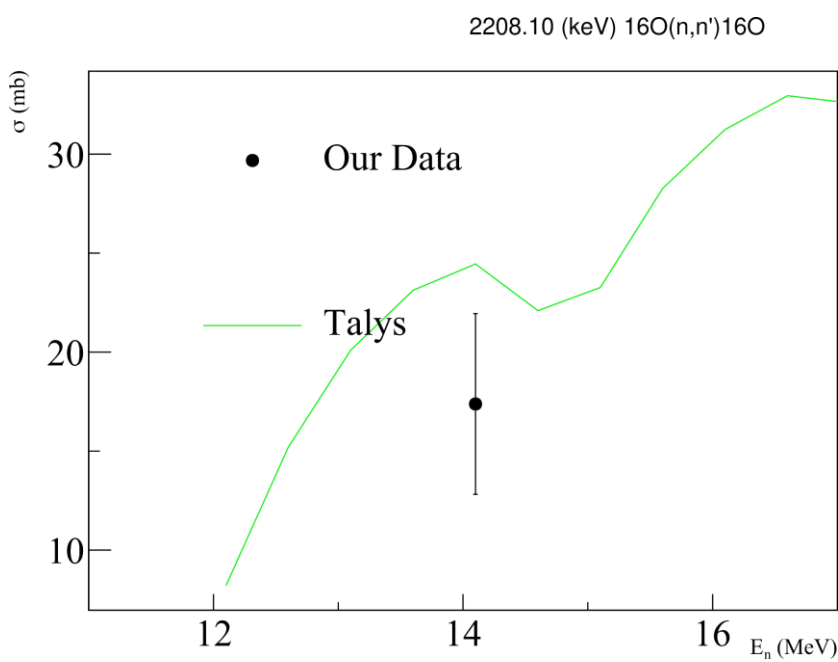
Angular distributions

6129.89 (keV) $^{16}\text{O}(n,n')^{16}\text{O}$



Ref.	a_2	a_4	a_6
Our Data $E_n: 14.1$ (MeV)	0.22 (0.11)	-0.08 (0.13)	-0.54 (0.16)
R.O.Nelson 2001 $E_n: 14.05$ (MeV)	0.40 (0.09)	-0.03 (0.12)	-0.70 (0.23)
T.Kozlowski 1965 $E_n: 14.10$ (MeV)	0.18 (0.32)	-0.27 (0.32)	-0.68 (0.48)

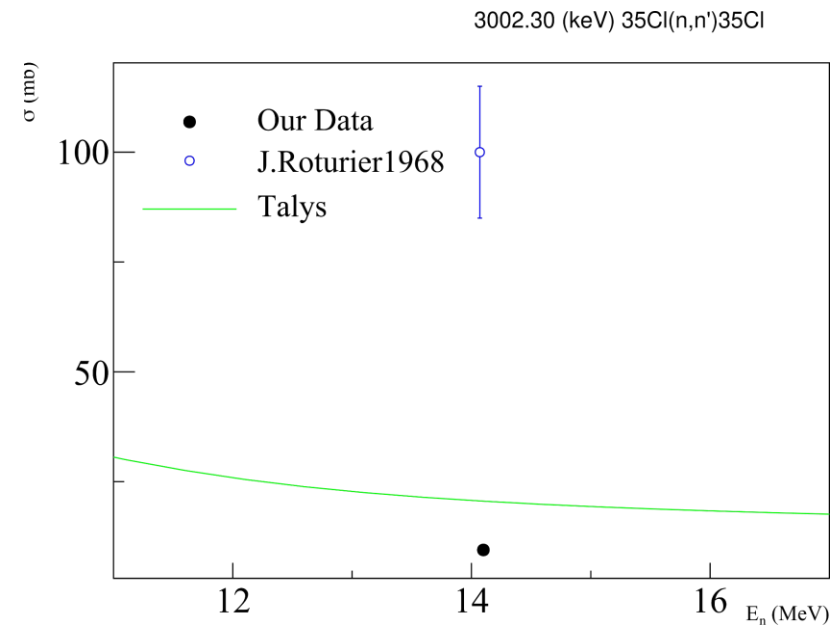
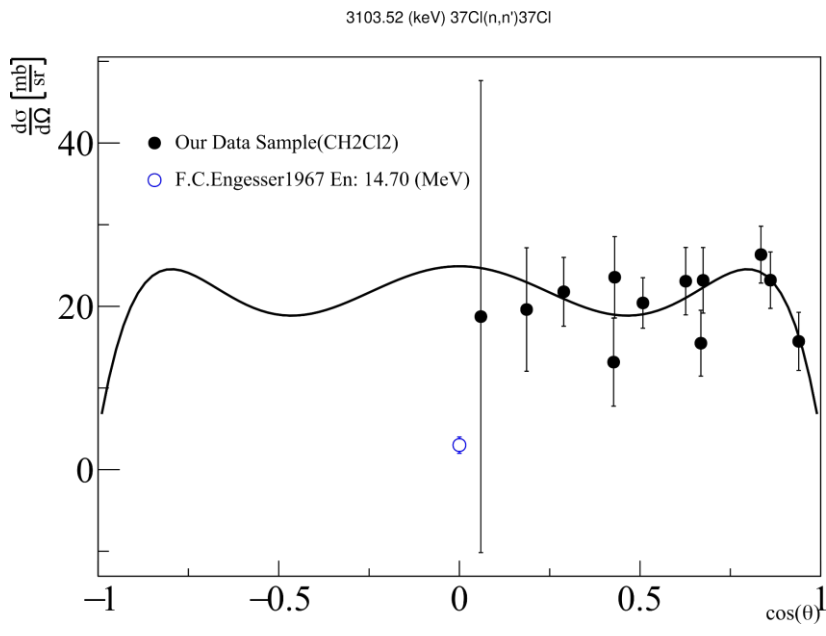
Results of cross-section measurements for oxygen



Results of cross-section measurements for oxygen

Energy (keV)	Reaction	σ (mb)		
		Our Data	Talys	Simakov
169	$^{16}\text{O}(\text{n},\alpha)^{13}\text{C}$	22 (5)	23	
298	$^{16}\text{O}(\text{n},\text{p})^{16}\text{N}$	31 (8)	23	
2208	$^{16}\text{O}(\text{n},\text{n}')^{16}\text{O}$	17 (5)	25	
2742	$^{16}\text{O}(\text{n},\text{n}')^{16}\text{O}$	18 (5)	51	38 (4)
3684	$^{16}\text{O}(\text{n},\alpha)^{13}\text{C}$	53 (13)	74	58 (5)
3853	$^{16}\text{O}(\text{n},\alpha)^{13}\text{C}$	29 (7)	40	34 (4)
6129	$^{16}\text{O}(\text{n},\text{n}')^{16}\text{O}$	114 (29)	132	148 (10)

Results of cross-section measurements for chlorine: Angular and Energy distributions



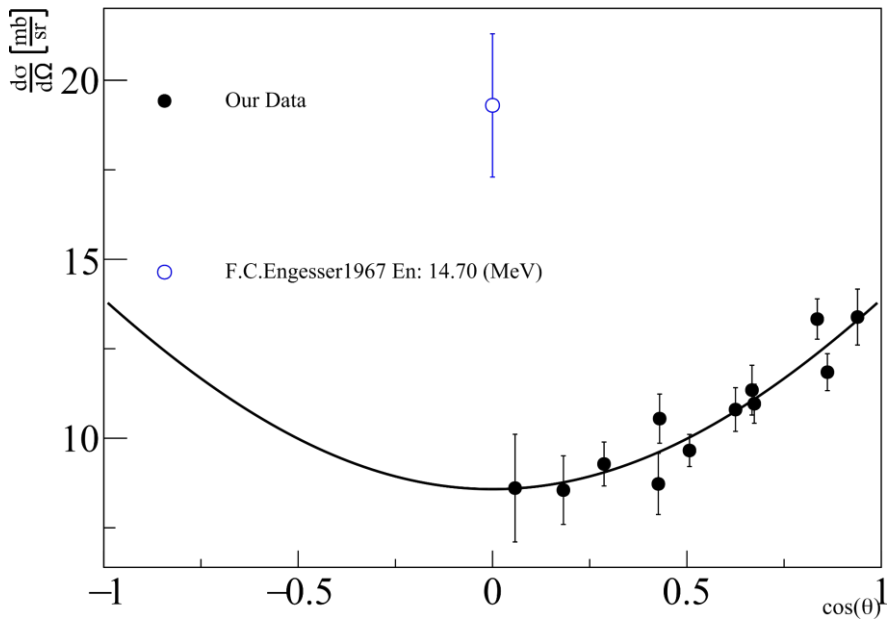
Results of cross-section measurements for chlorine

Energy (keV)	Reaction	σ (mb)		
		Our Data	Talys	Simakov
536	$^{37}\text{Cl}(\text{n},\text{n}')^{37}\text{Cl}$	51 (4)	27	
788	$^{37}\text{Cl}(\text{n},2\text{n})^{36}\text{Cl}$	142 (11)	175	
906	$^{37}\text{Cl}(\text{n},\text{n}')^{37}\text{Cl}$	74 (8)	47	
1164	$^{37}\text{Cl}(\text{n},2\text{n})^{36}\text{Cl}$	43 (3)	35	
1185	$^{35}\text{Cl}(\text{n},\text{n}')^{35}\text{Cl}$	57 (4)	15	
1219	$^{35}\text{Cl}(\text{n},\text{n}')^{35}\text{Cl}$	27 (2)	17	96 (20)
1266	$^{35}\text{Cl}(\text{n},\text{n}\alpha)^{31}\text{P}$	24 (4)	20	48 (16)
1676	$^{35}\text{Cl}(\text{n},\alpha)^{32}\text{P}$	43 (5)	26	

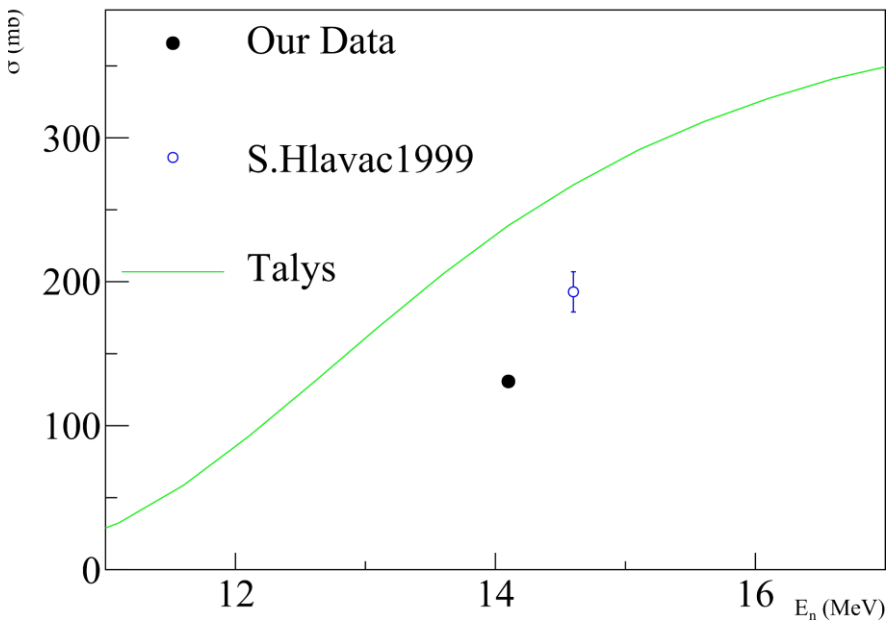
Energy (keV)	Reaction	σ (mb)		
		Our Data	Talys	Simakov
1726	$^{37}\text{Cl}(\text{n},\text{n}')^{37}\text{Cl}$	37 (10)	22	289 (90)
1763	$^{35}\text{Cl}(\text{n},\text{n}')^{35}\text{Cl}$	70 (6)	35	158 (43)
1991	$^{35}\text{Cl}(\text{n},\text{p})^{35}\text{S}$	34 (2)	17	
2645	$^{35}\text{Cl}(\text{n},\text{p})^{35}\text{S}$	43 (3)	35	
2645	$^{35}\text{Cl}(\text{n},\text{n}')^{35}\text{Cl}$	54 (4)	40	
3002	$^{35}\text{Cl}(\text{n},\text{n}')^{35}\text{Cl}$	9 (1)	20	
3103	$^{37}\text{Cl}(\text{n},\text{n}')^{37}\text{Cl}$	265 (19)	128	73 (15)

Results of cross-section measurements for potassium: Angular and Energy distributions

2167.47 (keV) $^{39}\text{K}(n,d)^{38}\text{Ar}$



2167.47 (keV) $^{39}\text{K}(n,d)^{38}\text{Ar}$



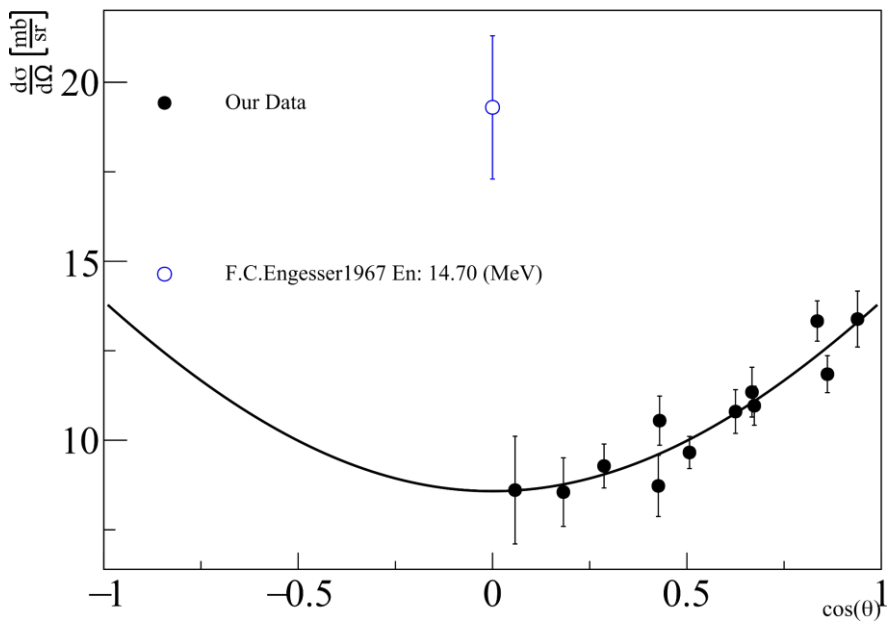
Results of cross-section measurements for potassium

Energy (keV)	Reaction	σ (mb)		
		Our Data	Talys	Simakov
346	$^{39}\text{K}(\text{n},\text{n}')^{39}\text{K}$	25 (2)	10	
669	$^{39}\text{K}(\text{n},\text{d})^{38}\text{Ar}$	22 (2)	26	
783	$^{39}\text{K}(\text{n},\text{n}')^{39}\text{K}$	105 (5)	22	
786	$^{39}\text{K}(\text{n},\alpha)^{36}\text{Cl}$	99 (5)	9	33 (24)
788	$^{39}\text{K}(\text{n},\alpha)^{36}\text{Cl}$	105 (5)	40	
923	$^{39}\text{K}(\text{n},\text{n}')^{39}\text{K}$	43 (3)	7	
1129	$^{39}\text{K}(\text{n},\text{n}')^{39}\text{K}$	25 (2)	18	
1164	$^{39}\text{K}(\text{n},\alpha)^{36}\text{Cl}$	25 (2)	32	21 (9)
1209	$^{39}\text{K}(\text{n},\text{d})^{38}\text{Ar}$	14 (1)	7	

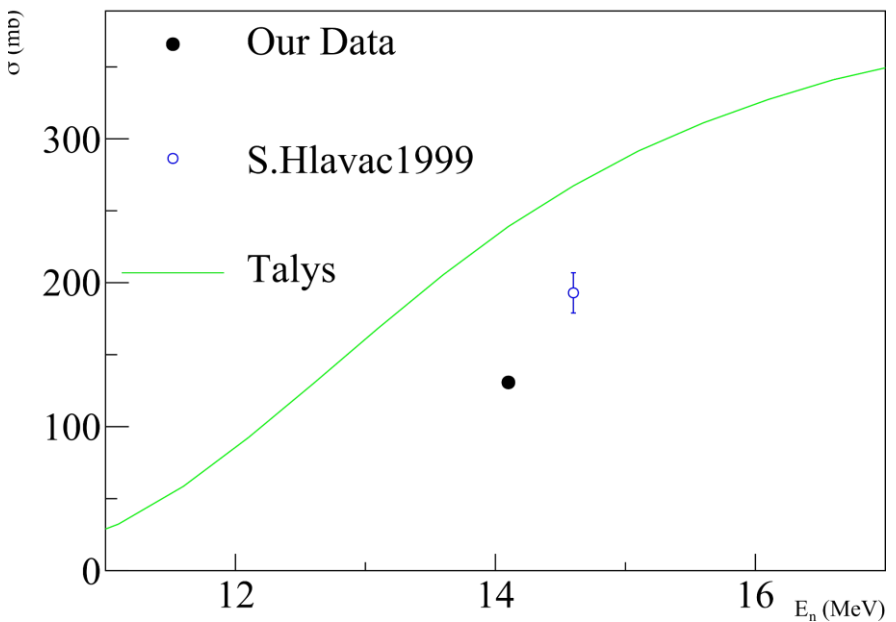
Energy (keV)	Reaction	σ (mb)		
		Our Data	Talys	Simakov
1267	$^{39}\text{K}(\text{n},\text{p})^{39}\text{Ar}$	19 (2)	16	22 (9)
1312	$^{39}\text{K}(\text{n},\text{n}')^{39}\text{K}$	18 (2)	23	
1642	$^{39}\text{K}(\text{n},\text{d})^{38}\text{Ar}$	56 (2)	55	
1677	$^{41}\text{K}(\text{n},\text{n}')^{41}\text{K}$	30 (5)	97	116 (11)
2167	$^{39}\text{K}(\text{n},\text{d})^{38}\text{Ar}$	130 (3)	240	218 (25)
2342	$^{39}\text{K}(\text{n},\text{p})^{39}\text{Ar}$	19 (2)	9	
2351	$^{39}\text{K}(\text{n},\text{n}')^{39}\text{K}$	19 (2)	6	
2814	$^{39}\text{K}(\text{n},\text{n}')^{39}\text{K}$	120 (5)	101	77 (8)
3597	$^{39}\text{K}(\text{n},\text{n}')^{39}\text{K}$	35 (2)	29	

Results of cross-section measurements for calcium: Angular and Energy distributions

2167.47 (keV) $^{39}\text{K}(\text{n},\text{d})^{38}\text{Ar}$



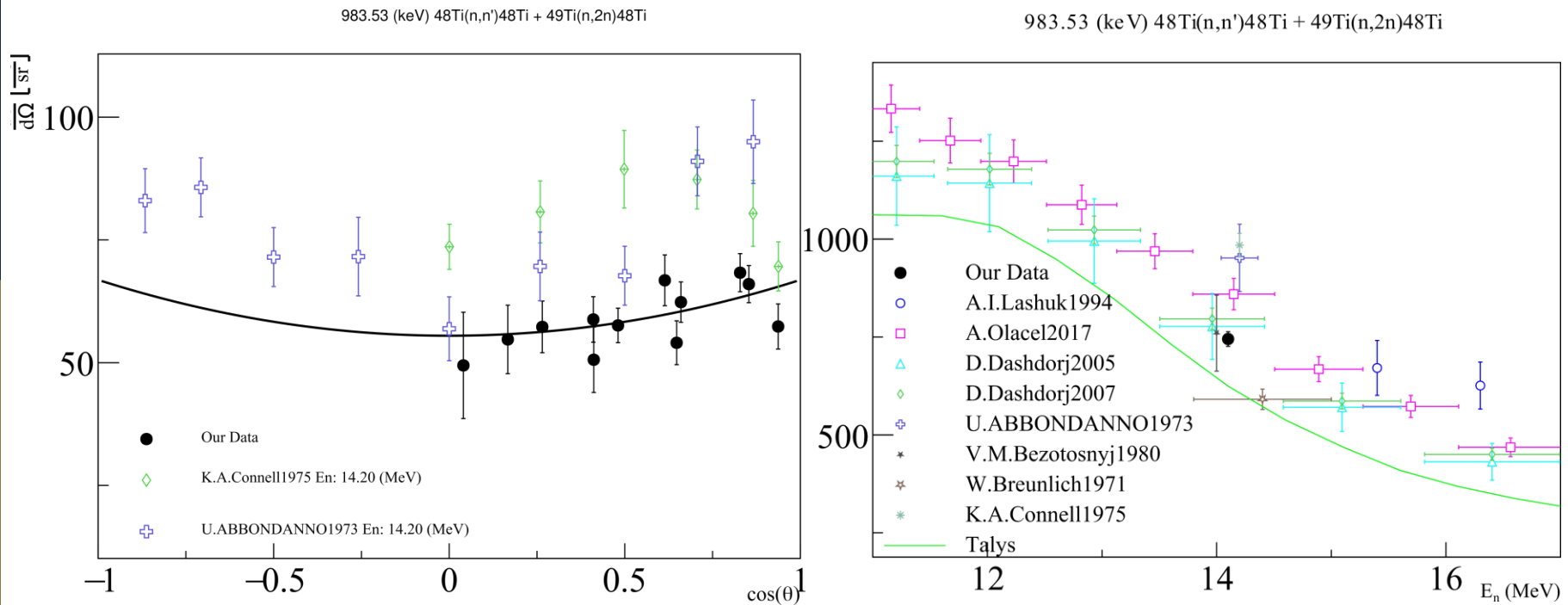
2167.47 (keV) $^{39}\text{K}(\text{n},\text{d})^{38}\text{Ar}$



Results of cross-section measurements for calcium

Energy (keV)	Reaction	σ (mb)		
		Our Data	Talys	Simakov
755	$^{40}\text{Ca}(\text{n},\text{n}')^{40}\text{Ca}$	87 (5)	37	
770	$^{40}\text{Ca}(\text{n},\text{p})^{40}\text{K}$	89 (5)	54	70 (15)
891	$^{40}\text{Ca}(\text{n},\text{p})^{40}\text{K}$	40 (3)	39	51 (16)
1158	$^{40}\text{Ca}(\text{n},\text{p})^{40}\text{K}$	18 (2)	10	28 (4)
1611	$^{40}\text{Ca}(\text{n},\alpha)^{37}\text{Ar}$	11 (2)	56	64 (12)
2217	$^{40}\text{Ca}(\text{n},\alpha)^{37}\text{Ar}$	16 (2)	20	
2814	$^{40}\text{Ca}(\text{n},\text{d})^{39}\text{K}$	27 (2)	18	
3736	$^{40}\text{Ca}(\text{n},\text{n}')^{40}\text{Ca}$	77 (5)	122	46 (11)

Results of cross-section measurements for titanium: Angular and Energy distributions



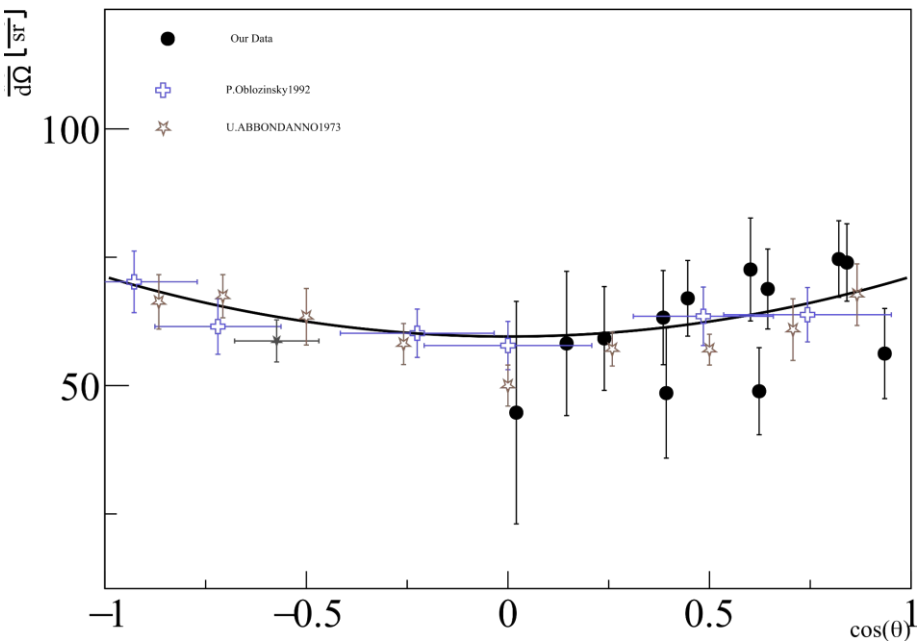
Cross-section measurement results of titanium

Energy (keV)	Reaction	σ (mb)		
		Our Data	Talys	Simakov
370	$^{48}\text{Ti}(\text{n},\text{p})^{48}\text{Sc}$	22 (2)	23	
889	$^{46}\text{Ti}(\text{n},\text{n}')^{46}\text{Ti}$ $^{47}\text{Ti}(\text{n},2\text{n})^{46}\text{Ti}$	536 (17)	681 585	62 (7)
944	$^{48}\text{Ti}(\text{n},\text{n}')^{48}\text{Ti}$	76 (4)	39	47 (6)
983	$^{48}\text{Ti}(\text{n},\text{n}')^{48}\text{Ti}$ $^{49}\text{Ti}(\text{n},2\text{n})^{48}\text{Ti}$	745 (19)	623 788	666 (61)
1037	$^{48}\text{Ti}(\text{n},\text{n}')^{48}\text{Ti}$ $^{49}\text{Ti}(\text{n},2\text{n})^{48}\text{Ti}$	92 (3)	65 163	49 (7)
1120	$^{48}\text{Ti}(\text{n},\text{n}')^{48}\text{Ti}$		334	
1120	$^{49}\text{Ti}(\text{n},2\text{n})^{48}\text{Ti}$	194 (6)	314	32 (4)
1121	$^{50}\text{Ti}(\text{n},\text{n}')^{50}\text{Ti}$		245	

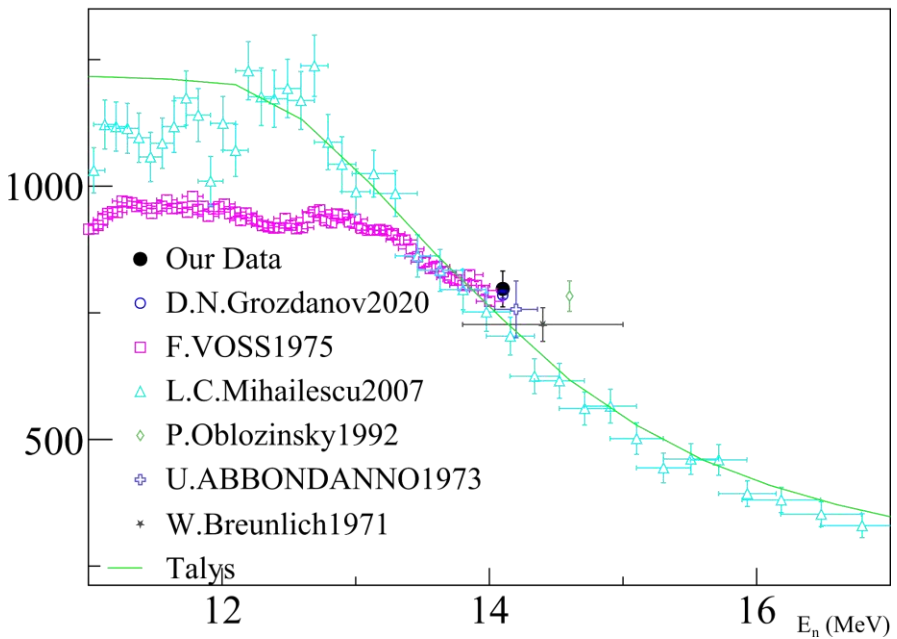
Energy (keV)	Reaction	σ (mb)		
		Our Data	Talys	Simakov
1312	$^{48}\text{Ti}(\text{n},\text{n}')^{48}\text{Ti}$ $^{49}\text{Ti}(\text{n},2\text{n})^{48}\text{Ti}$	350 (9)	263 444	238 (27)
1437	$^{48}\text{Ti}(\text{n},\text{n}')^{48}\text{Ti}$	60 (3)	36	49 (7)
1542	$^{49}\text{Ti}(\text{n},\text{n}')^{49}\text{Ti}$	450 (16)	148	32 (4)
2240	$^{48}\text{Ti}(\text{n},\text{n}')^{48}\text{Ti}$	35 (3)	23	32 (5)
2375	$^{48}\text{Ti}(\text{n},\text{n}')^{48}\text{Ti}$	88 (3)	55	57 (9)
2633	$^{48}\text{Ti}(\text{n},\text{n}')^{48}\text{Ti}$	38 (4)	9	

Results of cross-section measurements for chromium: Angular and Energy distribution

1434.09 (keV) $^{52}\text{Cr}(n,n')^{52}\text{Cr} + ^{53}\text{Cr}(n,2n)^{52}\text{Cr}$



1434.09 (keV) $^{52}\text{Cr}(n,n')^{52}\text{Cr} + ^{53}\text{Cr}(n,2n)^{52}\text{Cr}$

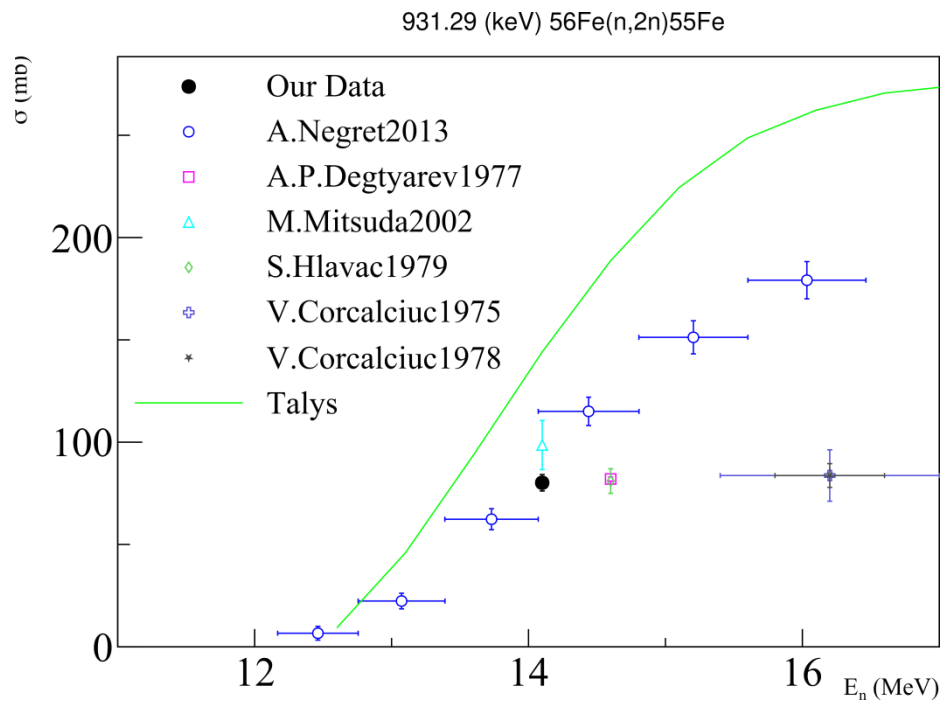
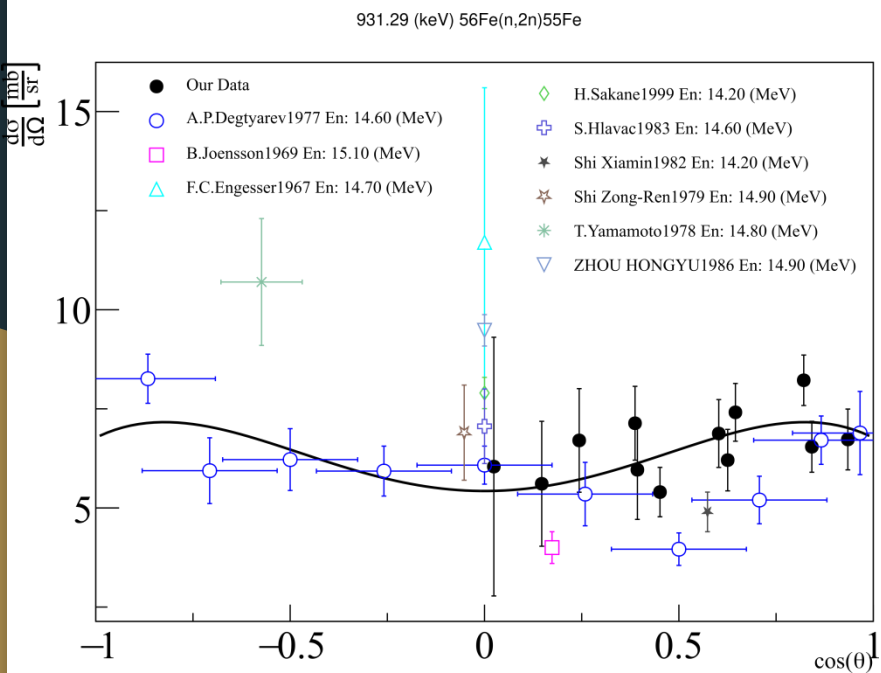


Results of cross-section measurements for chromium

Energy (keV)	Reaction	σ (mb)		
		Our Data	Talys	Simakov
320	$^{52}\text{Cr}(\text{n},\text{d})^{51}\text{V}$	8 (1)	13	
704	$^{52}\text{Cr}(\text{n},\text{n}')^{52}\text{Cr}$	50 (3)	30	29 (3)
783	$^{50}\text{Cr}(\text{n},\text{n}')^{50}\text{Cr}$	76 (4)	497	
848	$^{52}\text{Cr}(\text{n},\text{n}')^{52}\text{Cr}$	75 (5)	15	
935	$^{52}\text{Cr}(\text{n},\text{n}')^{52}\text{Cr}$	242 (10)	218	210 (9)
	$^{53}\text{Cr}(\text{n},2\text{n})^{52}\text{Cr}$		312	237 (9)
1006	$^{53}\text{Cr}(\text{n},\text{n}')^{53}\text{Cr}$	197 (15)	102	
	$^{54}\text{Cr}(\text{n},2\text{n})^{53}\text{Cr}$		279	23 (4)
1289	$^{53}\text{Cr}(\text{n},\text{n}')^{53}\text{Cr}$	63 (9)	139	
	$^{54}\text{Cr}(\text{n},2\text{n})^{53}\text{Cr}$		264	

Energy (keV)	Reaction	σ (mb)		
		Our Data	Talys	Simakov
1333	$^{52}\text{Cr}(\text{n},\text{n}')^{52}\text{Cr}$ $^{53}\text{Cr}(\text{n},2\text{n})^{52}\text{Cr}$	196 (9)	146 183	187 (13) 205 (8)
1434	$^{52}\text{Cr}(\text{n},\text{n}')^{52}\text{Cr}$ $^{53}\text{Cr}(\text{n},2\text{n})^{52}\text{Cr}$	797 (35)	708 826	695 (35) 783 (30)
1530	$^{52}\text{Cr}(\text{n},\text{n}')^{52}\text{Cr}$	62 (5)	39	40 (3)
1577	$^{52}\text{Cr}(\text{n},\text{n}')^{52}\text{Cr}$	13 (2)	12	
2337	$^{52}\text{Cr}(\text{n},\text{n}')^{52}\text{Cr}$	21 (2)	15	

Results of cross-section measurements for iron: Angular and Energy distribution



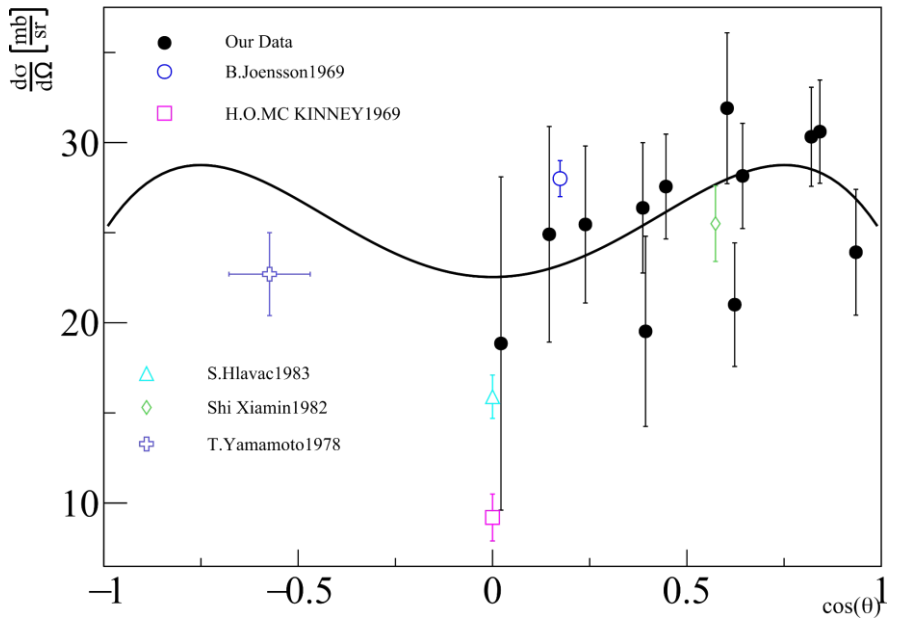
Results of cross-section measurements for iron

Energy (keV)	Reaction	σ (mb)		
		Our Data	Talys	Simakov
123	$^{56}\text{Fe}(\text{n},\text{p})^{56}\text{Mn}$	36 (4)	7	
125	$^{56}\text{Fe}(\text{n},\text{d})^{55}\text{Mn}$		28	70 (17)
211	$^{54}\text{Fe}(\text{n},\text{p})^{54}\text{Mn}$			
212	$^{56}\text{Fe}(\text{n},\text{p})^{56}\text{Mn}$	50 (3)	102	17 (1)
314	$^{56}\text{Fe}(\text{n},\text{p})^{56}\text{Mn}$	10 (1)	7	
367	$^{56}\text{Fe}(\text{n},\text{n}')^{56}\text{Fe}$	18 (2)	7	
378	$^{54}\text{Fe}(\text{n},\text{d})^{53}\text{Mn}$	280 (20)	153	
411	$^{56}\text{Fe}(\text{n},2\text{n})^{55}\text{Fe}$	31 (2)	55	53 (6)
477	$^{56}\text{Fe}(\text{n},2\text{n})^{55}\text{Fe}$	16 (2)	28	50 (7)
846	$^{56}\text{Fe}(\text{n},\text{n}')^{56}\text{Fe}$ $^{57}\text{Fe}(\text{n},2\text{n})^{56}\text{Fe}$	760 (42)	664 826	621 (29) 785 (48)
931	$^{56}\text{Fe}(\text{n},2\text{n})^{55}\text{Fe}$	80 (4)	144	126 (25)
1037	$^{56}\text{Fe}(\text{n},\text{n}')^{56}\text{Fe}$	71 (4)	54	52 (6)

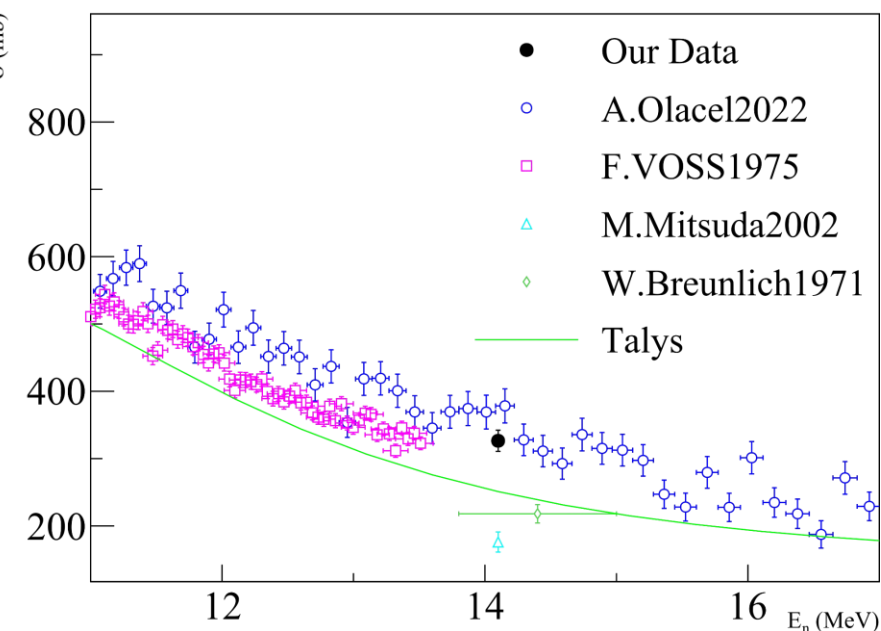
Energy (keV)	Reaction	σ (mb)		
		Our Data	Talys	Simakov
1238	$^{56}\text{Fe}(\text{n},\text{n}')^{56}\text{Fe}$ $^{57}\text{Fe}(\text{n},2\text{n})^{56}\text{Fe}$	366 (15)	319 369	393 (22) 290 (16)
1316	$^{56}\text{Fe}(\text{n},2\text{n})^{55}\text{Fe}$	139 (6)	59	54 (6)
1408	$^{56}\text{Fe}(\text{n},2\text{n})^{55}\text{Fe}$	31 (2)	24	24 (5)
1670	$^{56}\text{Fe}(\text{n},\text{n}')^{56}\text{Fe}$	45 (3)	31	55 (6)
1771	$^{56}\text{Fe}(\text{n},\text{n}')^{56}\text{Fe}$	45 (2)	11	
1810	$^{56}\text{Fe}(\text{n},\text{n}')^{56}\text{Fe}$	58 (2)	29	63 (5)
2113	$^{56}\text{Fe}(\text{n},\text{n}')^{56}\text{Fe}$	40 (3)	18	41 (6)
2523	$^{56}\text{Fe}(\text{n},\text{n}')^{56}\text{Fe}$	12 (2)	12	21 (5)
2598	$^{56}\text{Fe}(\text{n},\text{n}')^{56}\text{Fe}$	39 (3)	17	35 (5)
3002	$^{56}\text{Fe}(\text{n},\text{n}')^{56}\text{Fe}$	15 (2)	8	

Results of cross-section measurements for nickel: Angular and Energy distribution

1454.21 (keV) $^{58}\text{Ni}(n,n')^{58}\text{Ni}$



1454.21 (keV) $^{58}\text{Ni}(n,n')^{58}\text{Ni}$



Results of cross-section measurements for nickel

Energy (keV)	Reaction	σ (mb)		
		Our Data	Talys	Simakov
112	$^{58}\text{Ni}(\text{n},\text{p})^{58}\text{Co}$	21 (3)	37	
230	$^{60}\text{Ni}(\text{n},\text{p})^{60}\text{Co}$	137 (23)	41	
277	$^{60}\text{Ni}(\text{n},\text{p})^{60}\text{Co}$	9 (1)	39	
339	$^{60}\text{Ni}(\text{n},2\text{n})^{59}\text{Ni}$	180 (6)	126	
365	$^{58}\text{Ni}(\text{n},\text{p})^{58}\text{Co}$	24 (2)	43	
465*	$^{58}\text{Ni}(\text{n},\text{d})^{57}\text{Co}$	33 (3)	13	
467*	$^{60}\text{Ni}(\text{n},\text{n}')^{60}\text{Ni}$		47	
826	$^{60}\text{Ni}(\text{n},\text{n}')^{60}\text{Ni}$	104 (11)	138	25 (4)
931	$^{58}\text{Ni}(\text{n},\alpha)^{55}\text{Fe}$	46 (6)	46	29 (9)

Energy (keV)	Reaction	σ (mb)		
		Our Data	Talys	Simakov
1160*	$^{58}\text{Ni}(\text{n},\text{n}')^{58}\text{Ni}$			
1163*	$^{62}\text{Ni}(\text{n},\text{n}')^{62}\text{Ni}$			
1172*	$^{62}\text{Ni}(\text{n},\text{n}')^{62}\text{Ni}$			
1173*	$^{60}\text{Ni}(\text{n},\text{n}')^{60}\text{Ni}$			
1224	$^{58}\text{Ni}(\text{n},\text{d})^{57}\text{Co}$	458 (18)	92 (4)	76
1316	$^{58}\text{Ni}(\text{n},\alpha)^{55}\text{Fe}$	238 (11)	331 (15)	636
1332	$^{60}\text{Ni}(\text{n},\text{n}')^{60}\text{Ni}$	250	30	705
1454	$^{61}\text{Ni}(\text{n},2\text{n})^{60}\text{Ni}$	242 (27)	326 (16)	211 (24)
1787	$^{60}\text{Ni}(\text{n},\text{n}')^{60}\text{Ni}$	62	117 (9)	

Conclusion

As a result of the experiment, the applicability of the discussed setup for measuring cross sections and angular distributions was demonstrated.

The obtained data demonstrate satisfactory agreement with the results of the most recent measurements conducted by other authors.

**For the first time we measured cross sections for some lines with
O, Cl, K, Ca, Ti, Cr, Fe and Ni nuclea**

Thank you for your attention



Good team @ Good results